Since January 2020 Elsevier has created a COVID-19 resource centre with free information in English and Mandarin on the novel coronavirus COVID-19. The COVID-19 resource centre is hosted on Elsevier Connect, the company's public news and information website.

Journal of Ethnopharmacology 242 (2019) 111713

Contents lists available at ScienceDirect

Journal of Ethnopharmacology

journal homepage: www.elsevier.com/locate/jethpharm

Neutrophil elastase inhibitory effects of pentacyclic triterpenoids from *Eriobotrya japonica* (loquat leaves)

Jie Zhang[a], Hao-Yang Xu[b], Yu-Juan Wu[a], Xing Zhang[a], Liu-Qiang Zhang[a,*], Yi-Ming Li[a,*]

[a] School of Pharmacy, Shanghai University of Traditional Chinese Medicine, Shanghai 201203, China
[b] International Education College, Shanghai University of Traditional Chinese Medicine, Shanghai 201203, China

ARTICLE INFO

Keywords:
Loquat leaves
Pentacyclic triterpenoids
Human neutrophil elastase
Acute lung injury
Caco-2 cells

ABSTRACT

Ethnopharmacological relevance: *Eriobotrya japonica*, a traditional herbal medicine in China and Japan, has long been used to treat chronic bronchitis and coughs.

Aim of the study: Pentacyclic triterpenoids (PTs), especially ursolic acid (UA), have been found as reversibly and competitively human neutrophil elastase (HNE) inhibitors. However, the limited solubility and poor bioavailability of PTs hinder their clinical use. Crude plant extracts may have a greater activity than isolated constituents of the equivalent dosage. In this study, an *Eriobotrya japonica* (loquat leaves) extract (triterpenoid composition of loquat leaves, TCLL) with enriched PTs such as UA was prepared. The study aims to compare the HNE inhibitory (HNEI) effect *in vitro* and the therapeutic effect on acute lung injury (ALI) *in vivo* between TCLL and UA.

Materials and methods: An HNEI activity bioassay was performed with Sivelestat sodium hydrate as a positive control. A lipopolysaccharide (LPS)-induced lung inflammatory model was established to evaluate TCLL's therapeutic effect on ALI *in vivo*. The absorption of UA in TCLL and in UA alone was determined using a Caco-2 cell uptake model and LC-MS.

Results: The IC_{50} values of TCLL and UA for the HNEI effect were 3.26 ± 0.56 μg/mL and 8.49 ± 0.42 μg/mL ($P < 0.01$), respectively. TCLL significantly improved the inflammatory cells and inflammatory cytokine production in mice compared with the LPS group ($P < 0.05$). Additionally, it performed better than the UA alone group ($P < 0.05$). Moreover, the uptake by Caco-2 cells of UA in TCLL was higher than that in UA alone ($P < 0.05$).

Conclusion: TCLL has a significant HNEI effect *in vitro* and a therapeutic effect on LPS-induced inflammation in a mouse model. Both the effects are more efficient than UA. Improved absorption of PTs in TCLL may be one explanation for these results.

1. Introduction

Acute lung injury (ALI) is a syndrome comprising acute hypoxemic respiratory failure with bilateral pulmonary infiltrates, with a mortality rate of 40% and a cure rate of only 34% (Rubenfeld et al., 2005). This life-threatening disease can result from severe infections, shock, trauma, or burns (Tsai et al., 2015). Neutrophils are major inflammation mediators involved in the pathogenesis of various lung inflammatory diseases including ALI (Stevens et al., 2011). Neutrophilic inflammation has attracted considerable attention because of the influenza caused by the influenza A H1N1 and severe acute respiratory syndrome viruses (Yokoyama et al., 2010). Human neutrophil elastase (HNE) is a 30 kDa serine protease stored in the azurophilic granules of neutrophils. When inflammation occurs, HNE released from neutrophils and bound mainly to the neutrophil plasma membrane facilitates neutrophil migration to inflammation sites by degrading various host proteins, such as extracellular matrix proteins (Siedle et al., 2007). Under normal physiological conditions, HNE is controlled by its endogenous inhibitors (Fitch et al., 2006; Pham, 2006; Rubin, 1996; Williams et al., 2006). However, large amounts of oxygen radicals and proteases released by leukocytes recruited to inflammation sites can inactivate these endogenous inhibitors (Clark et al., 1981).

Abbreviations: PTs, Pentacyclic triterpenoids; UA, Ursolic acid; HNE, Human neutrophil elastase; TCLL, Triterpenoid composition of loquat leaves; LLs, Loquat leaves; LPS, Lipopolysaccharide; ALI, Acute lung injury; ^{1}H NMR, Proton nuclear magnetic resonance; HPLC, High-performance liquid chromatography; DEX, Dexamethasone; LC-MS, Liquid chromatography–mass spectrometry; BALF, Bronchoalveolar lavage fluid; DMSO, Dimethyl sulfoxide

* Corresponding authors.
E-mail addresses: jzhang258@163.com (J. Zhang), X13651886908@VIP.163.com (H.-Y. Xu), elena_wyj@163.com (Y.-J. Wu), zhangxing_1003@163.com (X. Zhang), 04100217@163.com (L.-Q. Zhang), ymli@mail.shutcm.edu.cn (Y.-M. Li).

https://doi.org/10.1016/j.jep.2019.01.037
Received 6 November 2018; Received in revised form 7 January 2019; Accepted 27 January 2019
Available online 28 January 2019

Environmental factors, including cigarette smoke and air pollution, and genetic factors can disrupt the protease-antiprotease balance (Brebner and Stockley, 2013; Cavarra et al., 2001; Gooptu and Lomas, 2009). Excess extracellular HNE can stimulate inflammatory lung disorders because of its involvement in inflammation, mucus overproduction, and lung tissue damage (Bergin et al., 2008; Caldwell et al., 2005; Wright et al., 2002).

Sivelestat sodium hydrate (ONO-5046) is the only clinically registered chemically synthesized HNE inhibitor approved for use in humans. It attenuates pulmonary disorders, improves pulmonary function, and is clinically used to treat pneumonia and ALI caused by viral infections (Yokoyama et al., 2010). However, ONO-5046 use is limited by its poor pharmacokinetics and the potential risk of organ toxicity because it irreversibly inhibits HNE by covalently binding to Ser-195 (Huang et al., 2008; Ohbayashi, 2002; Stevens et al., 2011). Research on synthetic HNE inhibitors has focused on nitrogen-containing heterocyclic compounds, among which AZD9668 has superior HNE selectivity to ONO-5046, with an IC_{50} value of 44 nM (Stevens et al., 2011). Compounds of the BAY series also inhibit HNE activity, with the IC_{50} value for the HNE inhibitory (HNEI) effect of BAY-678 at the picomolar level after structural modification. BAY-85–8501 was also effective in an ALI model in rodents (von Nussbaum et al., 2015). Moreover, natural terpenoids have been reported to possess an HNEI effect (Kim et al., 2015; Lee et al., 2015). In another study, we found that pentacyclic triterpenoids (PTs) protect against inflammation-induced lung injury by reversibly and competitively inhibiting HNE activity. Among these PTs, ursolic acid (UA) exhibited the highest inhibitory potency (IC_{50} = 5.51 μM) (Feng et al., 2013). However, its limited solubility and poor bioavailability hinder its practical use as a clinical drug (Liu, 2005).

Several strategies have been proposed to overcome this limitation, such as using suitable drug delivery systems (de Oliveira Eloy et al., 2012; Yang et al., 2014; Zhang et al., 2015). Evidence exists that crude plant extracts often have greater *in vitro* or *in vivo* activity than isolated constituents of the equivalent dosage (Rasoanaivo et al., 2011). We wanted to determine whether UA in a plant extract would have a better HNEI effect than purified UA and therefore chose *Eriobotrya japonica* (loquat leaves, LLs) as the objective material. In China and Japan, LLs have long been used as herbal medicine to treat chronic bronchitis and coughs (Cha et al., 2011). Studies have indicated many health-related benefits of LLs, including antioxidant and anti-inflammatory properties (Liu et al., 2016; Maher et al., 2015). LLs are also known to be abundant in PTs, including UA (Li et al., 2015). Therefore, this study elucidated the HNEI effect of the triterpenoid composition of loquat leaves (TCLL) compared with purified UA *in vitro* and *in vivo*.

2. Materials and methods

2.1. Chemicals and reagents

HNE (EC 3.4.21.37) from purulent human sputum was obtained (Innovative Research Company, Novi, MI, USA). HNE substrate (MeO-Suc-Ala-Ala-Pro-Val-pNA), soybean trypsin inhibitor, LPS, rhodamine 123, verapamil, and dimethyl sulfoxide (DMSO) were also obtained (Sigma, St. Louis, MO, USA) and used without further purification. Sivelestat sodium tetrahydrate (> 98.5%), euscaphic acid, maslinic acid, corosolic acid, oleanolic acid, and UA (> 98%) were purchased from Dalian Meilun Biotech Co., Ltd. (Dalian, China), and dexamethasone sodium phosphate for injection was purchased from Ma'anshan Fengyuan Pharmaceutical Co., Ltd. (Ma'anshan, Anhui, China). Chemicals and solvents for high-performance liquid chromatography (HPLC) and LC-MS were HPLC grade, whereas others used in this study were analytical grade.

2.2. Preparation of TCLL

LLs obtained in Guangdong Province, China, were extracted three times by using 85% ethanol, each time for 1 h. After the ethanol was removed under reduced pressure, the extract was centrifuged at 3000 rpm for 5 min. The supernatant was discarded, and the residues added sodium hydroxide (6.5% of the residues, g/g) were dissolved in a 15% ethanol water solution (50% of the residues, L/g). The mixture was heated at 70 °C for 10 min and then centrifuged at 3000 rpm for 10 min. Hydrochloric acid was added to the supernatant to adjust the pH of the solution to 6. Centrifuging was repeated, and the obtained residues constituted the final TCLL.

2.3. Fingerprint establishment of TCLL

The TCLL fingerprint was established through HPLC (Agilent Technologies, 1260, Santa Clara, CA, USA). The analytical column used was an Agilent Zorbax SB-C_{18} column (250 mm × 4.6 mm, 5 μm). The mobile phase comprised methanol, acetonitrile, and a 0.5% ammonium acetate water solution (45:35:20) with a flow rate of 1 mL/min. The compounds were monitored at 215 nm and kept at a column temperature of 25 °C. The TCLL sample was dissolved in methanol at 1 mg/mL.

2.4. TCLL compound identification

Compounds in TCLL were identified by comparing their retention time and MS ions with purchased standards and the compounds reported in literatures (UHPLC- LCQ Fleet ion trap MS system, Shimadzu, Kyoto, Japan for UHPLC and Thermo Fisher Scientific, Waltham, MA, USA for MS). Chromatographic separation was performed using the same method used for establishing the TCLL fingerprint. The sample solution was detected through MS with the ESI source in negative mode. The operational parameters of ESI-MS were as follows: the spray voltage was 5 kV; the vaporizer temperature was 300 °C; the sheath and aux gas pressure were 40 and 10 arbitrary units, respectively; and the capillary voltage was −35 V. A collision energy of 35 eV was used for the MS^2 fragments.

2.5. Determination of PTs in TCLL

The TCLL sample was prepared by dissolving an appropriate amount in methanol to produce a final concentration of 1 mg/mL. The solution was then analyzed through HPLC using the same method used for establishing the TCLL fingerprint. Following TCLL compound identification, euscaphic acid, maslinic acid, corosolic acid, oleanolic acid, and UA were used as external standards to calculate the total triterpenoid content of TCLL. Serial standard solutions at concentrations of 0.015, 0.03, 0.06, 0.125, 0.25, 0.5, and 1 mg/mL were injected to HPLC to plot the standard curves.

2.6. HNE activity inhibitory bioassay

An HNEI activity bioassay was performed as described (Feng et al., 2013). ONO-5046 was used as a positive control. Different concentrations of drugs (dissolved in DMSO) were added to a 200 μL substrate solution (1.4 mM MeO-Suc-Ala-Ala-Pro-Val-pNA in 10 mM Tris-HCl buffer; pH 7.5). After vortexing, 0.01 U of HNE enzyme was added, and the mixture was incubated for 1 h at 37 °C (protected from light). Then, 200 μL of soybean trypsin inhibitor (0.2 mg/mL) was added to the solution on ice to stop the interaction. 100 μL of each sample was placed in 96-well plate (3 auxiliary holes per sample), and measured at 405 nm using an automatic microplate reader (Bio-Tek, Synergy HT, Winooski, VT, USA). IC_{50} values were calculated through nonlinear fitting by using Graphpad Prism 5 software.

2.7. Animals

Male BALB/c mice (weight: 18–22 g) were obtained (Shanghai Laboratory Animal Co., Ltd., Shanghai, China). All of the mice were maintained in a 12-h light-dark cycle at a controlled temperature (22–23 °C) and relative humidity (50–60%). Food and water were provided ad libitum. All treatments were conducted according to the ethical guidelines for the care of laboratory animals approved by the ethics committee of Shanghai University of Traditional Chinese Medicine.

2.8. Experimental protocol

Fifty mice were randomly divided into five groups: control, LPS, dexamethasone (DEX, 3 mg/kg), UA (50 mg/kg), and TCLL (84 mg/kg). In total, 84 mg/kg of TCLL contains 50 mg/kg of total triterpenoids (59.6%), which was equivalent to the amount of UA in the UA group. Drugs were intragastrically administered to the mice once daily for 2 consecutive days (10% DMSO in double-distilled water for the control and LPS groups). One hour after the last drug administration, the control mice received saline and the others were intraperitoneally given 10 mg/kg LPS to induce acute lung inflammation. Six hours after LPS treatment, all of the mice were sacrificed. Lung tissues were excised, and blood samples and BALF were collected for analysis.

2.9. Collection of blood samples and BALF

After anesthetization, the heart and lungs of the mice were surgically exposed. Blood samples were collected from the heart. The lungs were lavaged three times through the tracheal cannula by using 0.5 mL of cold saline to obtain BALF. BALF and blood samples were centrifuged for 15 min at 3000 and 1,000 rpm for 15 min respectively. The supernatants were stored at −80 °C for analysis of inflammatory cytokine concentrations in the serum and BALF. The BALF cell pellet was re-suspended for measuring inflammatory cells.

2.10. Measurement of inflammatory cells and cytokines

Leukocyte and lymphocyte counts in blood samples and BALF were measured using an automated hematology analyzer (XS 500i, Sysmex Shanghai Ltd., Shanghai, China). TNF-α and IL-6 concentrations in serum and BALF were determined using commercially available enzyme-linked immunosorbent assay (ELISA) kits (mouse TNF-α and IL-6 ELISA Ready-SET-Go!, eBioscience, San Diego, CA, USA). All spectrophotometric readings were performed using an automatic microplate reader (Bio-Tek, Synergy HT, Winooski, VT, USA). All the experiments were performed in accordance with the manufacturers' instructions.

2.11. Histological examination

The left lung lobes were harvested and fixed in 4% paraformaldehyde for 1 week and then embedded in paraffin and stained using hematoxylin and eosin (H&E). Pulmonary pathological changes were observed under a microscope. A scoring system was used to evaluate lung injury, including pulmonary atelectasis, interstitial edema, alveolar hemorrhage, and inflammatory cell infiltration. Lung sections were scored according to the following criteria: 0 = no injury; 1 = slight injury (25%); 2 = moderate injury (50%); 3 = severe injury (75%); and 4 = very severe injury (almost 100%).

2.12. Cell culture

Caco-2 cells were obtained (American Type Culture Collection, Manassas, VA, USA), grown at 37 °C in an atmosphere of 5% CO_2 and 95% air, and cultivated in sterile Dulbecco's modified Eagle's medium (Mediatech Inc., Manassas, VA, USA) supplemented with 10% heat-inactivated fetal bovine serum (Biological Industries Inc., Cromwell, CT, USA). The culture medium was changed every 48 h until the cells grew to 85% confluence.

2.13. Uptake of UA in TCLL by Caco-2 cells

The uptake experiment was performed as described (Song et al., 2014). The Caco-2 cells were seeded in a 24-well plate and treated using UA (5 μM) or TCLL (18.5 μg/mL, containing 5 μM UA). The drugs were dissolved in DMSO and diluted using Hank's buffered salt solution (HBSS; Beyotime Institute of Biotechnology, Shanghai, China). Two hours later, the cells were washed using phosphate buffered saline and HBSS solution, and 0.1% Triton X-100 diluted in HBSS was added. The mixture was then sonicated for 20 min and centrifuged at 12,000 rpm for 20 min. The bicinchoninic acid (BCA) protein content in the pellet was measured using a BCA protein assay kit (Beyotime Institute of Biotechnology, Shanghai, China). 100 μL of supernatant with 700 μL of added acetonitrile was used to determine the UA concentration in the Caco-2 cells. After vortexing for 2 min, the mixture was centrifuged at 11,000 *g* for 10 min, and 5 μL of supernatant was analyzed through LC-MS.

2.14. LC-MS analysis of UA in Caco-2 cells

The UA concentration in Caco-2 cells was determined through LC-MS. An Ultimate 3000 UHPLC-TSQ triple quadrupole MS system (Thermo Fisher Scientific, Waltham, MA, USA) was equipped with a Zorbax Eclipse polyaromatic hydrocarbon column packed with 1.8 μm particles, 100 × 2.1 mm L_T × ID (Agilent Technologies, Santa Clara, CA, USA). The mobile phase comprised acetonitrile and ultra-pure water (70:30, v/v). The flow rate was 0.3 mL/min. The sample injection volume was 5 μL, with the column temperature kept at 30 °C.

Cell extracts were detected through MS with the ESI interface in negative selected-ion monitoring mode, monitoring the $[M–H]^-$ ion at *m/z* 455.4 for UA. The operational parameters of ESI-MS were as follows: the spray voltage was 2.5 kV; the vaporizer temperature was 350 °C; the sheath and aux gas pressure were 35 and 10 arbitrary units, respectively; and the capillary temperature was 350 °C.

2.15. Statistical analysis

All data were expressed as mean ± standard deviation. Data on the HNEI effect and uptake of UA by Caco-2 cells were analyzed using independent sample *t*-tests. Other data were analyzed through one-way analysis of variance followed by a Least Significant Difference *post hoc* test. All analyses were performed using SPSS 21.0.

3. Results

3.1. TCLL preparation, fingerprinting, and compound identification

TCLL and its fingerprint were obtained according to the procedures described in the Methods section. Eight peaks were detected in the TCLL fingerprint (Fig. 1). Peaks 1 and 5–8 were identified by comparing the retention time and ion information with standards through liquid chromatography-mass spectrometry (LC-MS Table 1). Therefore, it was confirmed that peak 1 is euscaphic acid and peaks 5–8 are maslinic acid, corosolic acid, oleanolic acid, and UA, respectively. The deprotonated ion (485.12) and MS^2 fragment ions (467.31 and 423.19) of peak 2 (Table 2) were consistent with the reported compound 2α, 19α-dihydroxy-3-oxo-urs-12-en-28-oic acid (with deprotonated ion 485.32, MS^2 fragment ions 467.32 and 423.33) (Wu et al., 2013). Moreover, the compound 2α, 19α-dihydroxy-3-oxo-urs-12-en-28-oic acid was isolated from LLs (Fig. 2, Tan et al., 2015).

The deprotonated ions and MS^2 fragment ions of peaks 3 and 4 were basically the same (Table 2, 633.27/487.06 for peak 3 and 633.15/

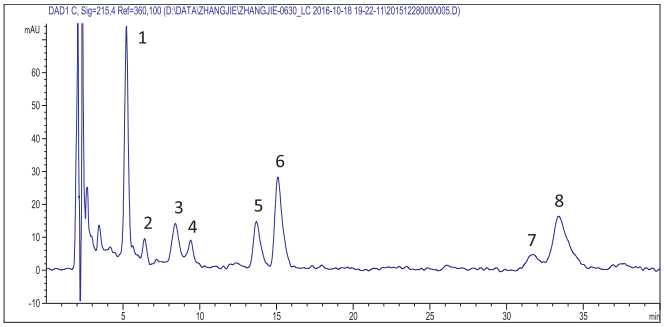

Fig. 1. Triterpenoid composition of loquat leaves (TCLL) fingerprint obtained through high-performance liquid chromatography (HPLC).

487.12 for peak 4) and consistent with the compound 3-*O*-*p*-coumaroyltormentic acid (633.38, 487.34, $[M–H–C_9H_6O_2]^-$) mentioned in the references (Cao et al., 2016; Tan et al., 2015; Wang et al., 2017; Wu et al., 2013). Peaks 3 and 4 were presumed to be the *cis* and *trans* isomers, respectively, of 3-*O*-*p*-coumaroyltormentic acid. Both were isolated from LLs (Tan et al., 2015). A mixture of peaks 3 and 4 was examined through nuclear magnetic resonance to obtain the ^{1}H NMR spectrum, where the area of peak 3 was significantly greater than that of peak 4. The ^{1}H NMR spectrum indicated the presence of *cis* and *trans* coumaroyl moieties, δ 7.65 (1H, *d*, J = 16 Hz) and δ 6.38 (1H, *d*, J = 15.9 Hz) for *trans* isomer, and δ 5.84 (1H, *d*, J = 12.8 Hz) for *cis* isomer (Taniguchi et al., 2002). When the peak area at δ 5.84 was scaled to 1, the peak area at δ 6.38 was 2.06, indicating that the content of the *trans*-structured compound in the mixture was approximately 2.06 times that of the *cis*-structured one. Peak 3 was confirmed as 3-*O*-*trans*-*p*-coumaroyltormentic acid, and peak 4 was confirmed as 3-*O*-*cis*-*p*-coumaroyltormentic acid.

3.2. TCLL content determination

The content of euscaphic acid, maslinic acid, corosolic acid, oleanolic acid, and UA was calculated as 14.5%, 6.0%, 11.6%, 5.3%, and 12.3% respectively according to the corresponding standard curves. The content of 2α, 19α-dihydroxy-3-oxo-urs-12-en-28-oic acid, 3-*O*-*trans*-*p*-coumaroyltormentic acid, and 3-*O*-*cis*-*p*-coumaroyltormentic acid calculated using the UA standard curve was 1.6%, 5.3%, and 2.9%, respectively. After calculation, the total PT content in TCLL was 59.6%.

3.3. HNE inhibitory effect of TCLL in vitro

The HNEI effect of TCLL was examined using an HNE *in vitro* activity assay. The positive control ONO-5046 had an IC_{50} value of 266.87 ± 45.10 nM. UA and TCLL could both inhibit HNE activity, with a maximum inhibition of approximately 60% in this assay. The IC_{50} value of TCLL was 3.26 ± 0.56 μg/mL, which was significantly lower than that of UA (8.49 ± 0.42 μg/mL, $P < 0.01$, Table 3 and Fig. 3). TCLL thus had a superior HNEI effect *in vitro* to UA.

3.4. Effects of TCLL on inflammatory cells in blood and bronchoalveolar lavage fluid (BALF) of lipopolysaccharide (LPS)-induced ALI mice

To evaluate the effect of TCLL on ALI, leukocytes and lymphocytes in blood and leukocytes in BALF were counted. The doses of TCLL and UA were 84 mg/kg and 50 mg/kg, respectively, such that the dose of total PTs in TCLL equaled that of UA in the UA group. Six hours after LPS injection, leukocytes in blood and BALF and lymphocytes in blood significantly decreased ($P < 0.01$), whereas TCLL increased leukocytes ($P < 0.01$) and lymphocytes ($P < 0.05$) in blood and leukocytes ($P < 0.01$) in BALF. However, the leukocytes and lymphocytes in blood and BALF in the UA group mice did not significantly differ from those in the LPS group ($P > 0.05$, Fig. 4).

3.5. Effects of TCLL on inflammatory cytokine production in serum and BALF of LPS-induced ALI mice

After LPS injection, levels of TNF-α and IL-6 in serum and IL-6 in BALF significantly increased ($P < 0.01$). TCLL reduced levels of TNF-α and IL-6 in serum and IL-6 in BALF ($P < 0.01$, Fig. 5). However, the serum TNF-α level in the UA group was significantly higher than in the TCLL group ($P < 0.01$, Fig. 5a), indicating that the effect of UA in decreasing serum TNF-α was weaker than that of TCLL.

3.6. Effects of TCLL on LPS-mediated histological changes in lung tissues

Histological changes in lung tissues were observed through light microscopy to examine the therapeutic effect of TCLL on lung injury. No evident histological alteration was observed in the control group. LPS administration caused obvious pathological changes such as alveolar wall thickening and collapse, inflammatory cell infiltration, congestion, and edema. TCLL treatment significantly attenuated the histological changes induced by LPS, whereas UA treatment did not significantly reduce the destructive effects of lung injury (Fig. 6a–e). Lung injury scores are presented in Fig. 6f. The results indicated that TCLL could reduce the degree of pathological inflammation in lung tissues in ALI, with an effect superior to that of UA.

3.7. UA uptake in TCLL by Caco-2 cells

The UA uptake by Caco-2 cells in the UA and TCLL groups was examined through LC-MS. The UA dose was equal in both groups (5 μM). However, the UA uptake in the TCLL group was significantly greater than in the UA group ($P < 0.05$, Fig. 7). The results indicated that UA uptake by Caco-2 cells could be promoted in a mixture state involving various triterpenoids.

4. Discussion

LLs have been used since ancient times to treat inflammatory diseases such as cough, chronic bronchitis, and asthma. Extracts from LLs are reportedly abundant in triterpenoids and possess anti-inflammatory effects through suppression of nuclear factor-κB expression and activation (Cha et al., 2011; Kim and Shin, 2009; Kwon et al., 2000; Lee et al., 2008; Uto et al., 2010) and the mitogen-activated protein kinase signaling pathway (Huang et al., 2009; Kim and Shin, 2009; Uto et al.,

Table 1
Comparison of retention time and MS ions of peak 1 and peaks 5–8 with standards in negative full-scan mode.

Compound/peak	Retention time (min)	MS ions (*m/z*)
euscaphic acid peak 1	5.40/5.38	546.47, 974.60/545.48, 974.58
maslinic acid/peak 5	13.91/13.87	530.53, 942.36/530.62, 942.54
corosolic acid/peak 6	15.25/15.30	530.04, 942.51/530.18, 942.46
oleanolic acid/peak 7	31.80/31.69	514.45, 933.09, 1410.75/514.41, 933.08, 1410.67
UA/peak 8	33.55/33.59	514.46, 933.23, 1410.82/514.34, 933.17, 1410.86

Table 2
$[M–H]^-$ and MS^2 ions of peaks 2–4 in negative mode.

Peak	$[M-H]^-$ (*m/z*)	MS^2 ions (*m/z*)	Identified compounds	Ref.
peak 2	485.12	467.31, 423.19, 393.38	2α,19α-dihydroxy-3-oxo-urs-12-en-28-oic acid	(Tan et al., 2015; Wu et al., 2013)
peak 3	633.27	487.06 ($[M–H–C_9H_6O_2]^-$)	3-*O-trans-p*-coumaroyltormentic acid	(Cao et al., 2016; Tan et al., 2015; Wang et al., 2017; Wu et al., 2013)
peak 4	633.15	487.12 ($[M–H–C_9H_6O_2]^-$)	3-*O-cis-p*-coumaroyltormentic acid	(Cao et al., 2016; Tan et al., 2015; Wang et al., 2017; Wu et al., 2013)

2010). In this study, the anti-pulmonary-inflammation effect of the extract was proved to be related to the HNEI effect.

Using relatively simple methods, we obtained TCLL, an extract of LLs abundant in PTs. TCLL contains eight of the main PTs in LLs, including UA. The results indicated that TCLL had a significant HNEI effect *in vitro* and a therapeutic effect on LPS-induced inflammation in a mouse model. Specifically, TCLL significantly increased leukocyte counts and reduced inflammatory cytokines (TNF-α and IL-6) in blood and BALF. The histological changes induced by LPS were also significantly attenuated by TCLL. Furthermore, the data showed that TCLL had a lower IC_{50} value for HNEI effect *in vitro* and was more effective in treating ALI *in vivo* than UA.

A twofold explanation may explain why TCLL performed superiorly: *In vitro*, certain PTs or other constituents of TCLL might have a stronger HNEI effect than UA, whereas *in vivo* a pharmacodynamic synergistic effect or pharmacokinetic interactions of PTs in TCLL might occur.

Table 3
IC_{50} values of UA and TCLL.

Sample	IC_{50}
ONO-5046	266.87 ± 45.10 nM
UA	8.49 ± 0.42 μg/mL
TCLL	3.26 ± 0.56 μg/mL*

* Significantly different from UA group ($P < 0.01$).

P-glycoprotein (P-gp) is one of the major human transmembrane transporters (Zhou, 2008) and decreases the oral bioavailability of many drugs that are its substrates through an efflux mechanism (Eckford and Sharom, 2009). Some studies have reported that PTs are likely to be substrates for P-gp. When a solid dispersion of total PTs in

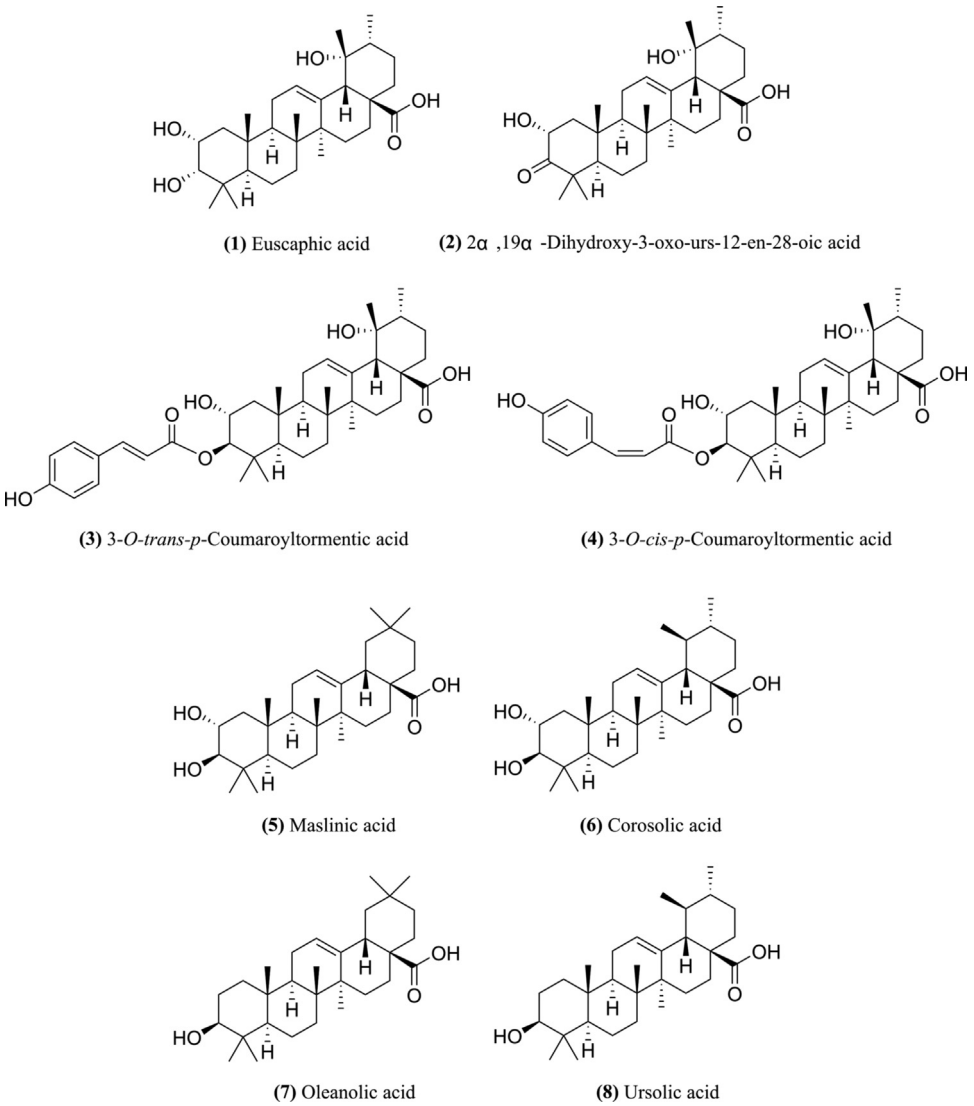

Fig. 2. Structure of the eight compounds in TCLL.

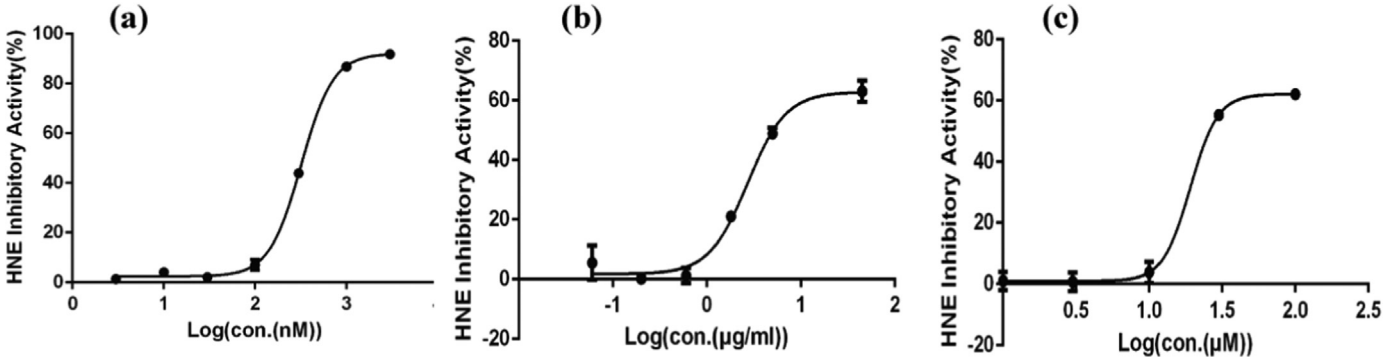

Fig. 3. Curve of human neutrophil elastase (HNE) inhibitory activity (n = 3): (a) ONO-5046; (b) TCLL; (c) Ursolic acid (UA).

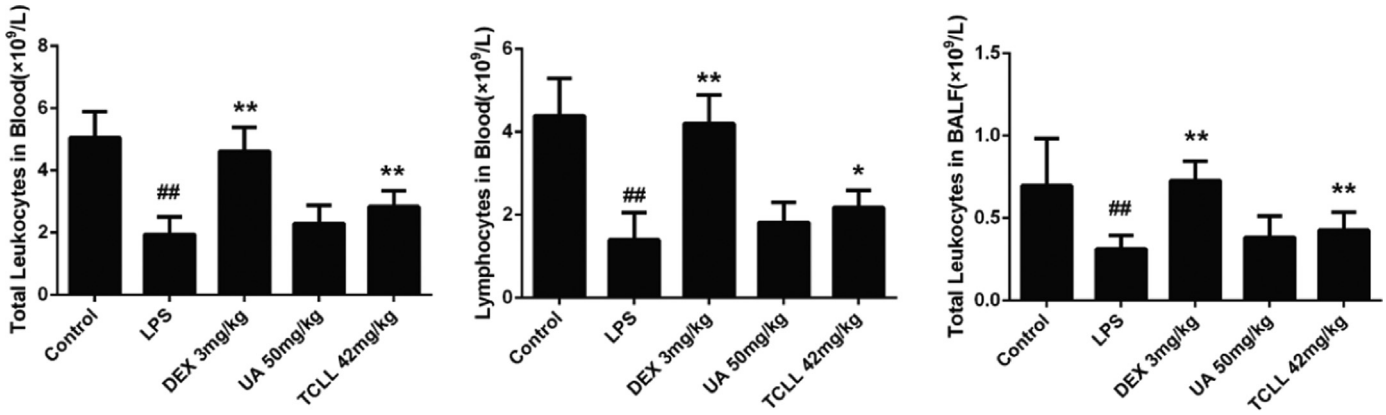

Fig. 4. Effects of TCLL on inflammatory cells in blood and bronchoalveolar lavage fluid (BALF) of lipopolysaccharide (LPS)-induced acute lung injury (ALI) mice: (a) total leukocytes in blood; (b) lymphocytes in blood; (c) total leukocytes in BALF. Data are presented as mean ± SD (n = 8–10). $^{\#\#}$ P < 0.01 compared with control group; * P < 0.05, ** P < 0.01 compared with LPS group.

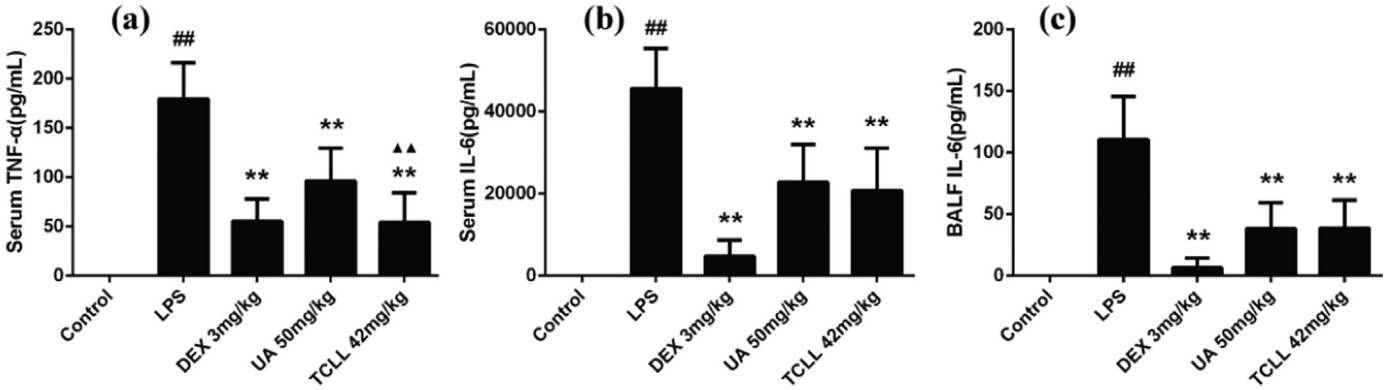

Fig. 5. Effects of TCLL on the production of inflammatory cytokines in serum and BALF of LPS-induced ALI mice: (a) TNF-α levels in serum; (b) IL-6 levels in serum; (c) IL-6 levels in BALF. Data are presented as mean ± SD (n = 8–10). $^{\#\#}$ P < 0.01 compared with control group; * P < 0.05, ** P < 0.01 compared with LPS group; ▲▲P < 0.01 compared with UA group.

LLs containing euscaphic acid, maslinic acid, corosolic acid, oleanolic acid, and UA was co-administered with the P-gp inhibitor verapamil in a rat model, the relative bioavailability of these PTs increased (Cai, 2013). In this study, UA uptake in TCLL was performed by Caco-2 cells, with the results indicating that UA uptake by Caco-2 cells in TCLL was higher than that in UA alone. The results demonstrated that PTs in TCLL, which are likely to be P-gp substrates, can compete with each other in binding to P-gp, thereby increasing UA uptake in Caco-2 cells.

UA is one of the major active components of LLs. Along with its HNEI and anti-inflammatory activity, UA has many other pharmacological properties (Wozniak et al., 2015), including anticancer, antioxidant, and antibacterial activity. In this study, we demonstrated that TCLL had an enhanced HNEI effect as well as a therapeutic effect on LPS-induced inflammation. Because TCLL is simple and inexpensive to prepare, LLs extracts could replace UA in other pharmacological applications.

CRediT authorship contribution statement

Y.-M. Li, **L.-Q. Zhang**: Project administration, Writing - review & editing. **J. Zhang**: Data curation, Writing - original draft. **H.-Y. Xu**: Formal analysis. **Y.-J. Wu**, **X. Zhang**: Methodology.

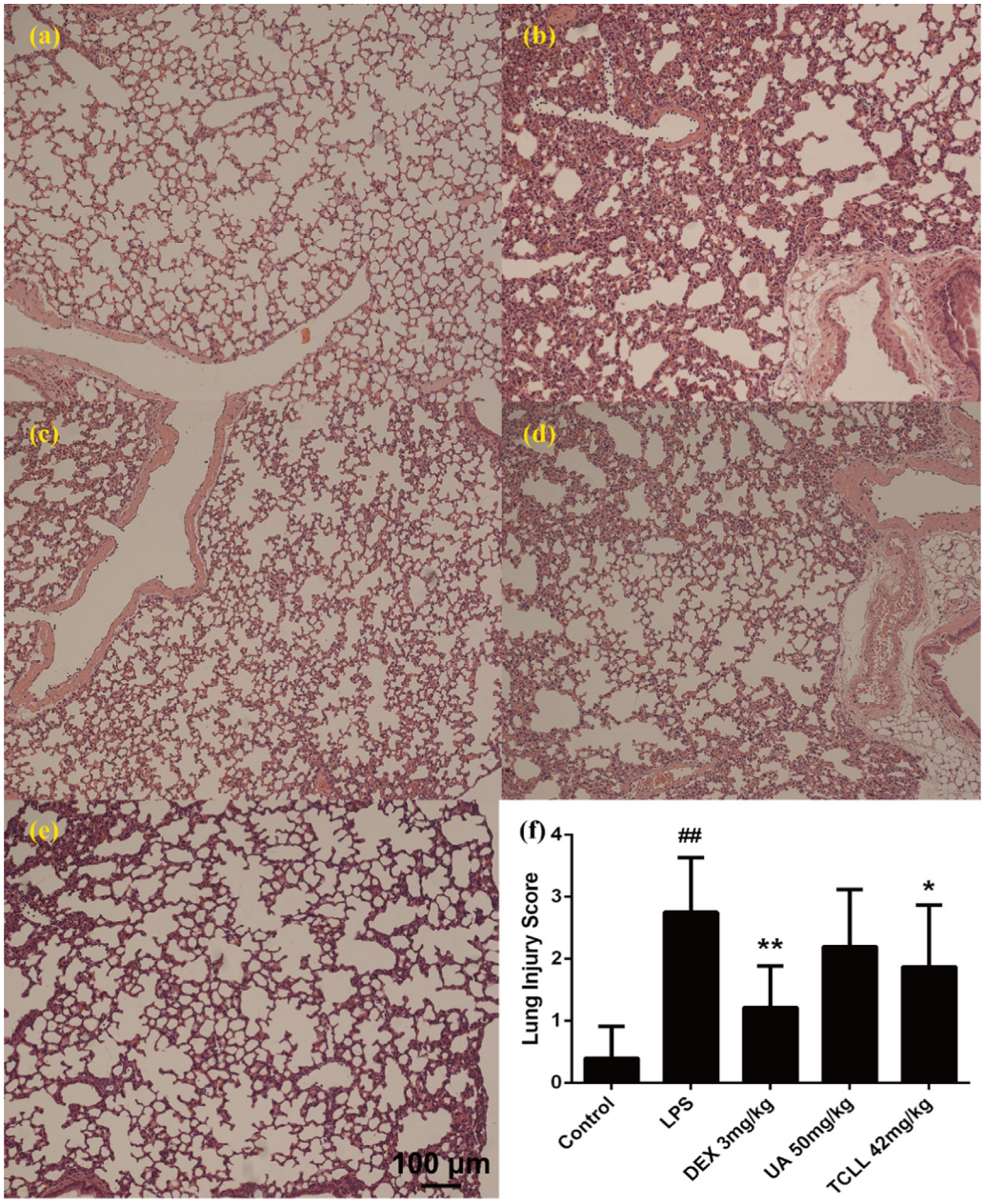

Fig. 6. Effects of TCLL on LPS-mediated histological changes in lung tissues (hematoxylin and eosin, H&E stain, ×100): (a) control group; (b) LPS group; (c) dexamethasone (DEX) 3 mg/kg group; (d) UA 50 mg/kg group; (e) TCLL 84 mg/kg group; (f) lung injury score. Data are presented as mean ± SD (n = 10). ## P < 0.01 compared with control group; * P < 0.05, ** P < 0.01 compared with LPS group.

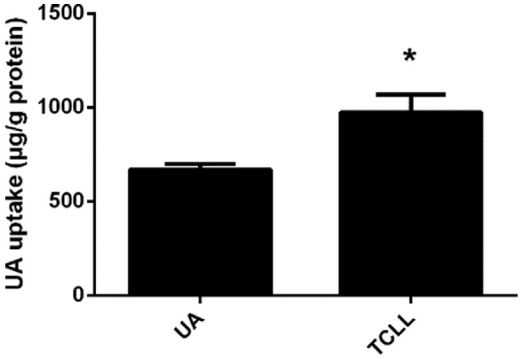

Fig. 7. Uptake of UA in TCLL by Caco-2 cells. Data are presented as mean ± SD (n = 4). * P < 0.05 compared with UA group.

Acknowledgments

This research was supported by the National Natural Science Foundation of China (81673570), the Excellent Academic Leaders Program of Shanghai (16XD1403500), the Shanghai Science and Technology Innovation Action Plan (18401931100), and the Program of Shanghai E-Research Institute of Bioactive Constituents in Traditional Chinese Medicine.

Conflicts of interest

The authors declare no conflict of interest.

Appendix A. Supplementary material

Supplementary data associated with this article can be found in the

online version at doi:10.1016/j.jep.2019.01.037.

References

Bergin, D.A., Greene, C.M., Sterchi, E.E., Kenna, C., Geraghty, P., Belaaouaj, A., Taggart, C.C., O'Neill, S.J., McElvaney, N.G., 2008. Activation of the epidermal growth factor receptor (EGFR) by a novel metalloprotease pathway. J. Biol. Chem. 283 (46), 31736–31744.

Brebner, J.A., Stockley, R.A., 2013. Recent advances in alpha-1-antitrypsin deficiency-related lung disease. Expert Rev. Respir. Med. 7 (3), 213–229 (quiz 230).

Cai, X.P., 2013. Study on Solid Dispersion Tablet of Triterpenoid Acids Effective Fraction from Leaves of Eriobotrya japonica. Nanjing University of Chinese Medicine, Nanjing, China.

Caldwell, R.A., Boucher, R.C., Stutts, M.J., 2005. Neutrophil elastase activates near-silent epithelial Na^+ channels and increases airway epithelial Na^+ transport. American journal of physiology. Lung Cell. Mol. Physiol. 288 (5), L813–L819.

Cao, J., Peng, L.Q., Xu, J.J., 2016. Microcrystalline cellulose based matrix solid phase dispersion microextration for isomeric triterpenoid acids in loquat leaves by ultra-high-performance liquid chromatography and quadrupole time-of-flight mass spectrometry. J. Chromatogr. A 1472, 16–26.

Cavarra, E., Bartalesi, B., Lucattelli, M., Fineschi, S., Lunghi, B., Gambelli, F., Ortiz, L.A., Martorana, P.A., Lungarella, G., 2001. Effects of cigarette smoke in mice with different levels of alpha(1)-proteinase inhibitor and sensitivity to oxidants. Am. J. Respir. Crit. Care Med. 164 (5), 886–890.

Cha, D.S., Eun, J.S., Jeon, H., 2011. Anti-inflammatory and antinociceptive properties of the leaves of Eriobotrya japonica. J. Ethnopharmacol. 134 (2), 305–312.

Clark, R.A., Stone, P.J., El Hag, A., Calore, J.D., Franzblau, C., 1981. Myeloperoxidase-catalyzed inactivation of alpha 1-protease inhibitor by human neutrophils. J. Biol. Chem. 256 (7), 3348–3353.

de Oliveira Eloy, J., Saraiva, J., de Albuquerque, S., Marchetti, J.M., 2012. Solid dispersion of ursolic acid in Gelucire 50/13: a strategy to enhance drug release and trypanocidal activity. AAPS PharmSciTech 13 (4), 1436–1445.

Eckford, P.D., Sharom, F.J., 2009. ABC efflux pump-based resistance to chemotherapy drugs. Chem. Rev. 109 (7), 2989–3011.

Feng, L., Liu, X., Zhu, W., Guo, F., Wu, Y., Wang, R., Chen, K., Huang, C., Li, Y., 2013. Inhibition of human neutrophil elastase by pentacyclic triterpenes. PLoS One 8 (12), e82794.

Fitch, P.M., Roghanian, A., Howie, S.E., Sallenave, J.M., 2006. Human neutrophil elastase inhibitors in innate and adaptive immunity. Biochem. Soc. Trans. 34 (Pt 2), 279–282.

Gooptu, B., Lomas, D.A., 2009. Conformational pathology of the serpins: themes, variations, and therapeutic strategies. Annu. Rev. Biochem. 78, 147–176.

Huang, W., Yamamoto, Y., Li, Y., Dou, D., Alliston, K.R., Hanzlik, R.P., Williams, T.D., Groutas, W.C., 2008. X-ray snapshot of the mechanism of inactivation of human neutrophil elastase by 1,2,5-thiadiazolidin-3-one 1,1-dioxide derivatives. J. Med. Chem. 51 (7), 2003–2008.

Huang, Y., Li, J., Meng, X.M., Jiang, G.L., Li, H., Cao, Q., Yu, S.C., Lv, X.W., Cheng, W.M., 2009. Effect of triterpene acids of Eriobotrya japonica (Thunb.) Lindl. leaf and MAPK signal transduction pathway on inducible nitric oxide synthase expression in alveolar macrophage of chronic bronchitis rats. Am. J. Chin. Med. 37 (6), 1099–1111.

Kim, K.C., Lee, I.S., Yoo, I.D., Ha, B.J., 2015. Sesquiterpenes from the fruiting bodies of Ramaria formosa and their human neutrophil elastase inhibitory activity. Chem. Pharm. Bull. 63 (7), 554–557.

Kim, S.H., Shin, T.Y., 2009. Anti-inflammatory effect of leaves of Eriobotrya japonica correlating with attenuation of p38 MAPK, ERK, and NF-kappaB activation in mast cells. Toxicol. Vitr.: Int. J. Publ. Assoc. BIBRA 23 (7), 1215–1219.

Kwon, H.J., Kang, M.J., Kim, H.J., Choi, J.S., Paik, K.J., Chung, H.Y., 2000. Inhibition of NFkappaB by methyl chlorogenate from Eriobotrya japonica. Mol. Cells 10 (3), 241–246.

Lee, C.H., Wu, S.L., Chen, J.C., Li, C.C., Lo, H.Y., Cheng, W.Y., Lin, J.G., Chang, Y.H., Hsiang, C.Y., Ho, T.Y., 2008. Eriobotrya japonica leaf and its triterpenes inhibited lipopolysaccharide-induced cytokines and inducible enzyme production via the nuclear factor-kappaB signaling pathway in lung epithelial cells. Am. J. Chin. Med. 36 (6), 1185–1198.

Lee, I.S., Kim, K.C., Yoo, I.D., Ha, B.J., 2015. Inhibition of human neutrophil elastase by labdane diterpenes from the fruiting bodies of Ramaria formosa. Biosci. Biotechnol. Biochem. 79 (12), 1921–1925.

Li, Z.H., Zhu, H., Cai, X.P., He, D.D., Hua, J.L., Ju, J.M., Lv, H., Ma, L., Li, W.L., 2015. Simultaneous determination of five triterpene acids in rat plasma by liquid chromatography-mass spectrometry and its application in pharmacokinetic study after oral administration of Folium Eriobotryae effective fraction. Biomed. Chromatogr.: BMC 29 (12), 1791–1797.

Liu, J., 2005. Oleanolic acid and ursolic acid: research perspectives. J. Ethnopharmacol. 100 (1–2), 92–94.

Liu, Y., Zhang, W., Xu, C., Li, X., 2016. Biological activities of extracts from loquat (Eriobotrya japonica Lindl.): a review. Int. J. Mol. Sci. 17 (12).

Maher, K., Yassine, B.A., Sofiane, B., 2015. Anti-inflammatory and antioxidant properties of Eriobotrya japonica leaves extracts. Afr. Health Sci. 15 (2), 613–620.

Ohbayashi, H., 2002. Neutrophil elastase inhibitors as treatment for COPD. Expert Opin. Investig. Drugs 11 (7), 965–980.

Pham, C.T., 2006. Neutrophil serine proteases: specific regulators of inflammation. Nat. Rev. Immunol. 6 (7), 541–550.

Rasoanaivo, P., Wright, C.W., Willcox, M.L., Gilbert, B., 2011. Whole plant extracts versus single compounds for the treatment of malaria: synergy and positive interactions. Malar. J. 10 (Suppl. 1), S4.

Rubenfeld, G.D., Caldwell, E., Peabody, E., Weaver, J., Martin, D.P., Neff, M., Stern, E.J., Hudson, L.D., 2005. Incidence and outcomes of acute lung injury. New Engl. J. Med. 353 (16), 1685–1693.

Rubin, H., 1996. Serine protease inhibitors (SERPINS): where mechanism meets medicine. Nat. Med. 2 (6), 632–633.

Siedle, B., Hrenn, A., Merfort, I., 2007. Natural compounds as inhibitors of human neutrophil elastase. Planta Med. 73 (5), 401–420.

Song, Q., Li, D., Zhou, Y., Yang, J., Yang, W., Zhou, G., Wen, J., 2014. Enhanced uptake and transport of (+)-catechin and (-)-epigallocatechin gallate in niosomal formulation by human intestinal Caco-2 cells. Int. J. Nanomed. 9, 2157–2165.

Stevens, T., Ekholm, K., Granse, M., Lindahl, M., Kozma, V., Jungar, C., Ottosson, T., Falk-Hakansson, H., Churg, A., Wright, J.L., Lal, H., Sanfridson, A., 2011. AZD9668: pharmacological characterization of a novel oral inhibitor of neutrophil elastase. J. Pharmacol. Exp. Ther. 339 (1), 313–320.

Tan, H., Ashour, A., Katakura, Y., Shimizu, K., 2015. A structure-activity relationship study on antiosteoclastogenesis effect of triterpenoids from the leaves of loquat (Eriobotrya japonica). Phytomed.: Int. J. Phytother. Phytopharm. 22 (4), 498–503.

Taniguchi, S., Imayoshi, Y., Kobayashi, E., Takamatsu, Y., Ito, H., Hatano, T., Sakagami, H., Tokuda, H., Nishino, H., Sugita, D., Shimura, S., Yoshida, T., 2002. Production of bioactive triterpenes by Eriobotrya japonica calli. Phytochemistry 59 (3), 315–323.

Tsai, Y.F., Yu, H.P., Chang, W.Y., Liu, F.C., Huang, Z.C., Hwang, T.L., 2015. Sirtinol inhibits neutrophil elastase activity and attenuates lipopolysaccharide-mediated acute lung injury in mice. Sci. Rep. 5, 8347.

Uto, T., Suangkaew, N., Morinaga, O., Kariyazono, H., Oiso, S., Shoyama, Y., 2010. Eriobotryae folium extract suppresses LPS-induced iNOS and COX-2 expression by inhibition of NF-kappaB and MAPK activation in murine macrophages. Am. J. Chin. Med. 38 (5), 985–994.

von Nussbaum, F., Li, V.M., Allerheiligen, S., Anlauf, S., Barfacker, L., Bechem, M., Delbeck, M., Fitzgerald, M.F., Gerisch, M., Gielen-Haertwig, H., Haning, H., Karthaus, D., Lang, D., Lustig, K., Meibom, D., Mittendorf, J., Rosentreter, U., Schafer, M., Schafer, S., Schamberger, J., Telan, L.A., Tersteegen, A., 2015. Freezing the bioactive conformation to boost potency: the identification of BAY 85-8501, a selective and potent inhibitor of human neutrophil elastase for pulmonary diseases. ChemMedChem 10 (7), 1163–1173.

Wang, J., Jia, Z., Zhang, Z., Wang, Y., Liu, X., Wang, L., Lin, R., 2017. Analysis of chemical constituents of Melastoma dodecandrum Lour. by UPLC-ESI-Q-Exactive focus-MS/MS. Molecules 22 (3).

Williams, S.E., Brown, T.I., Roghanian, A., Sallenave, J.M., 2006. SLPI and elafin: one glove, many fingers. Clin. Sci. (Lond. Engl.: 1979) 110 (1), 21–35.

Wozniak, L., Skapska, S., Marszalek, K., 2015. Ursolic acid – a pentacyclic triterpenoid with a wide spectrum of pharmacological activities. Molecules 20 (11), 20614–20641.

Wright, J.L., Farmer, S.G., Churg, A., 2002. Synthetic serine elastase inhibitor reduces cigarette smoke-induced emphysema in guinea pigs. Am. J. Respir. Crit. Care Med. 166 (7), 954–960.

Wu, L., Jiang, X., Huang, L., Chen, S., 2013. Processing technology investigation of loquat (Eriobotrya japonica) leaf by ultra-performance liquid chromatography-quadrupole time-of-flight mass spectrometry combined with chemometrics. PLoS One 8 (5), e64178.

Yang, G., Yang, T., Zhang, W., Lu, M., Ma, X., Xiang, G., 2014. In vitro and in vivo antitumor effects of folate-targeted ursolic acid stealth liposome. J. Agric. Food Chem. 62 (10), 2207–2215.

Yokoyama, T., Tsushima, K., Ushiki, A., Kobayashi, N., Urushihata, K., Koizumi, T., Kubo, K., 2010. Acute lung injury with alveolar hemorrhage due to a novel swine-origin influenza A (H1N1) virus. Intern. Med. 49 (5), 427–430.

Zhang, H., Zheng, D., Ding, J., Xu, H., Li, X., Sun, W., 2015. Efficient delivery of ursolic acid by poly(N-vinylpyrrolidone)-block-poly (epsilon-caprolactone) nanoparticles for inhibiting the growth of hepatocellular carcinoma in vitro and in vivo. Int. J. Nanomed. 10, 1909–1920.

Zhou, S.F., 2008. Structure, function and regulation of P-glycoprotein and its clinical relevance in drug disposition. Xenobiotica; Fate Foreign Compd. Biol. Syst. 38 (7–8), 802–832.